Mathematical Biosciences and Engineering

MBE, 18(6): 7060–7075.
DOI: 10.3934/mbe.2021351
Received: 30 June 2021
Accepted: 12 August 2021
Published: 24 August 2021

http://www.aimspress.com/journal/MBE

Research article

Principal stress lines based design method of lightweight and low vibration amplitude gear web

Ganjun Xu[1], Ning Dai[1,*] and Sukun Tian[2]

[1] National Key Laboratory of Science and Technology on Helicopter Transmission, Nanjing University of Aeronautics and Astronautics, Nanjing 210016, China
[2] School of Mechanical Engineering, Shandong University, Jinan 250061, China

* **Correspondence:** Email: dai_ning@nuaa.edu.cn.

Abstract: A lightweight and low vibration amplitude web design method was investigated to reduce gear weight and noise. It was based upon the relationship between length and orthogonality that the principal stress lines were designed at the gear web. By constructing a vibration control model with gear design parameters, the optimal distance was calculated. By offsetting the principal stress lines at the optimal distance, the lightweight gear web with the low vibration amplitude was then generated. A vibration experimental platform was built to verify the novel gear vibration performances, and it was compared with other gears with the same web's porosity to verify loading performance. The experimental results indicated that compared with the solid gear, the novel gear is 20.50% lighter and with a 29.46% vibration amplitude reduction.

Keywords: principal stress line; porous web; optimal shape; lightweight; low vibration amplitude

1. Introduction

The helicopter's flight speed and load capacity are affected by its weight, vibration and noise levels. Therefore, how to minimize their impact is the main goal to improve the high-performance transmission system. Based upon the traditional mechanical design methods, some gear parts in the helicopters are often designed conservatively to maintain higher mechanical performance. However, it results in that a portion of the gear web has an area of excessively low stress while the adjacent areas already reach the stress limit. This stress imbalance indicates that in theory the gear design has room

for improvement with the application of lightweight design [1]. In the traditional gear weight reduction design, it is typically done by adjusting the gear web's thickness [2] or creating the spoke structure [3]. They will reduce the gear weight but will not improve the vibration performance or reduce the noise level. The vibration reduction design on the gear parts is important in theoretical and engineering fields.

During the gear meshing, the continuous change in the gear tooth's stiffness makes it a vibration source [4]. Many researchers focused on two ways to enhance the gear's vibration performance: the gear tooth profile modification and the gear web structure optimization. Ghosh et al. [5] explored to optimize the gear tooth profile modification under varying conditions such as different speed and load. The results indicated that the gear tooth profile modification would be conductive to the gear's vibration performance only at high speed. Handschuh et al. [6] designed a gear with the composite materials. The results revealed that compared with the all-metallic gear, this composite gear's weight decreased by 20% but with a better damping performance. Xiao et al. [7] proposed a design filling eight fixed circular opening regions on the gear web with the spherical damping materials and evaluated its vibration performance with an energy dissipation model. The findings indicated that the proposed design could achieve obvious gear vibration reduction. Ramadani et al. [8] designed a lattice porous gear with a weight reduction of 58.8% that could also reduce the noise level. By comparing solid structure design with porous structure design, Li et al. [9] found that the latter could increase the acoustic energy loss due to the structural internal friction by increasing the noise travelling distance and changing the direction multiple times among its path. Hence the vibration performance of the structure would be improved. The above research suggests that a porous gear web can improve the gear vibration performance, but it should also possess certain strength and stiffness to meet the loading performance.

In the latest trend of porous structural design, researchers are applying Topology Optimization and structural principal stress lines design. The principle of Topology Optimization is to maximize the natural frequency of the model while control the structure weight [10]. Whereas, there are two problems in the implementation of this method: (a) meshing in Finite Element Analysis is difficult [11]; (b) the precision of model reconstruction after optimization is difficult to control [12], which results in the dilemma that Topology optimization can't be applied to all parts design. On the other hand, as a forward parametric modeling method, structural principal stress lines design is based on the principle that the structural materials are distributed along its principal stress lines [13]. Principal stress lines can predict the ultimate destructive force of the structure as well as its fracture path. Hence designing the porous structure around the structural principal stress lines can make structure lighter while ensuring enough structural stiffness [14]. Xu et al. [15] proposed a method to transform Topology Optimization design into structural principal stress lines design. The design variables of porous structure are reduced, simplifying the subsequent mathematical optimization model.

In this research, an innovative design method of gear web was explored using parametric porous structural design. Based upon the principal stress lines design, the gear web was designed as a porous structure. By applying the vibration control model, the web's porosity adjustment would improve its vibration performance to achieve the optimal results, while the gear was able to maintain sufficient loading performance. The findings indicate that this new gear web design method can reduce the gear weight and significantly improve its vibration performance.

2. Workflow overview

The workflow overview of this research is described in two steps below:

(I) Lightweight and low vibration amplitude gear web design. The goal is to design a porous web, whose materials are distributed along its principal stress lines. The design workflow is shown in Figure 1, based on the relationship of length and orthogonality, the principal stress lines are constructed at the gear web. By constructing the vibration control model with gear design parameters, the optimal distance will be calculated. By offsetting the principal stress lines at the optimal distance, the lightweight gear web with low vibration amplitude will be generated.

(II) Experimental design and analysis. A vibration experimental platform was built to detect the vibration and loading performance of the gear with the porous web: (a) In the vibration experiment, hold vibration amplitude as the criterion and evaluate the vibration performance. (b) In the loading experiment, hold the motor's output torque till the gear is broken as the criterion and evaluate the loading performance.

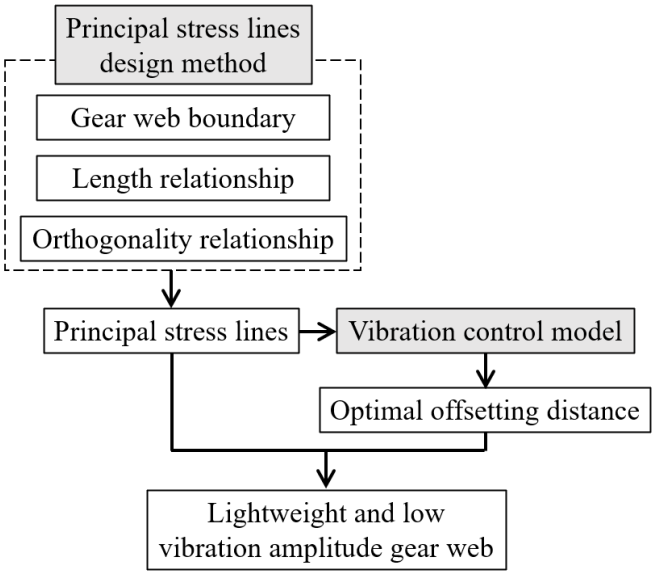

Figure 1. Design workflow of the lightweight and low vibration amplitude gear web.

3. Design method

3.1. Porous web model

By increasing the noise travelling distance and changing the direction multiple times along its path, the porous structure can effectively reduce vibration level. Therefore, applying the porous structural design method into gear web design can reduce the gear weight and improve the gear vibration performance. By removing materials in the low stress region and preserving materials in the high stress region, Topology Optimization was applied to porous web design [15]. As shown in Figure 2, after Topology Optimization of the solid gear, a porous web, whose materials are distributed along the principal stress lines of the gear web, was constructed. Inspired by this phenomenon, the porous web design method based on structural principal stress lines was explored, whose goal is to reduce the gear weight while maintaining sufficient loading performance.

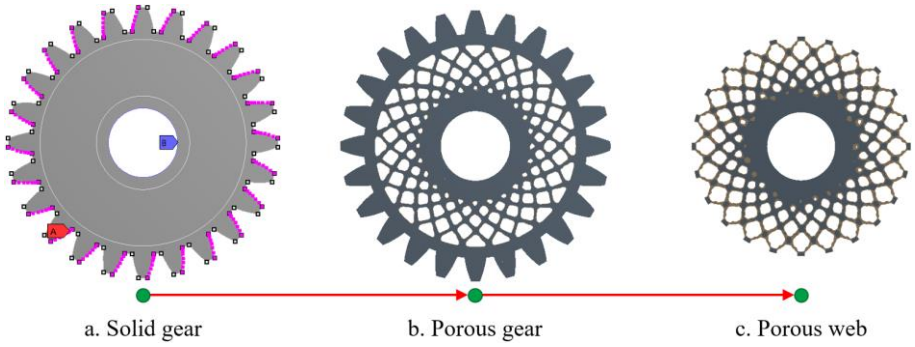

Figure 2. Porous web model.

3.2. Principal stress lines design method

The design workflow is shown in Figure 3. According to the gear's loading condition, the loads are transferred from each outer gear tooth to the inner hub. The goal is to construct principal stress lines at the gear web. This method is divided into three steps: (a) According to the relationships of Length and Orthogonality, a group of concentric circles with proportioned radiuses are constructed at the gear web. (b) According to the number of the gear teeth z, the concentric circles are uniformly divided by its radius lines, and the longest tensile lines will be obtained by connecting the intersection points. (c) Array the longest tensile lines around the gear web, and the overall principal stress lines will be generated.

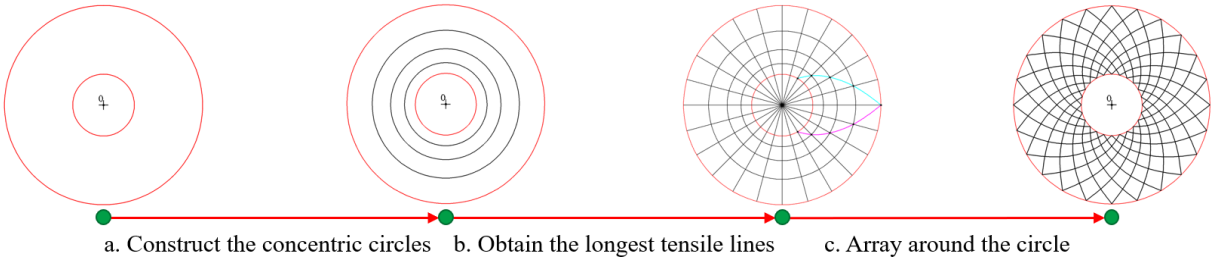

Figure 3. Design workflow of principal stress lines design.

3.2.1. Length relationship

As depicted in Figure 4(a), if and only if the principal stress lines are proportional, they will get the shortest length and the largest span 16. As shown in Figure 4(b), the principal stress lines P_0P_1, P_1P_2, P_2P_3, P_3P_4, with the length of l_1, l_2, l_3, l_4, are constructed in five concentric circles with the radius of r_0, r_1, r_2, r_3, r_4. Then, four similar triangles which are $\triangle OP_0P_1$, $\triangle OP_1P_2$, $\triangle OP_2N_3$, $\triangle OP_3P_4$ are formed by the above four principal stress lines and lines OP_0, OP_1, OP_2, OP_3, OP_4. According to the property of similar triangles, when l_1, l_2, l_3, l_4 have a multiple relationship, r_0, r_1, r_2, r_3, r_4 also have a multiple relationship. Thus, the length relationship expression can be developed with variables of α and θ. Where α equals $2\pi/z$.

$$\frac{l_{n+1}}{l_n}=\frac{r_{n+1}}{r_n}=\frac{\sin\theta}{\sin(\theta+\alpha)} \tag{1}$$

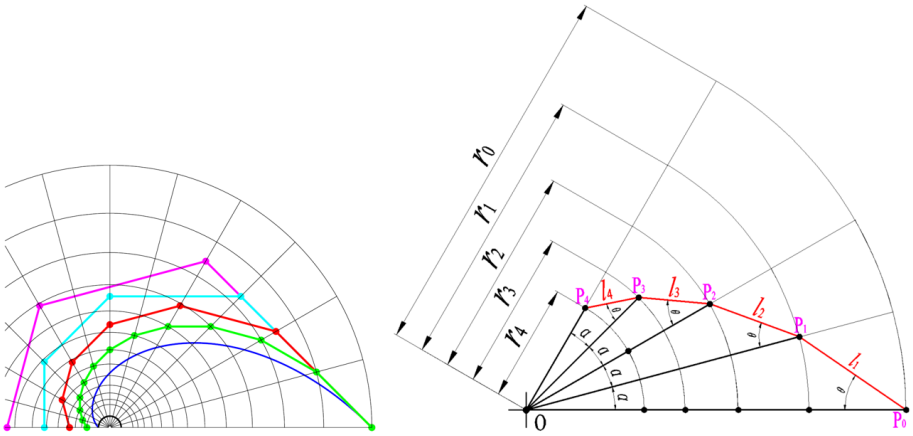

(a) Principal stress lines which are proportional 16, (b) Principal line design in this section

Figure 4. Length relationship.

3.2.2. Orthogonality relationship

As depicted in Figure 5(a), if and only if γ equals $\pi/2$, the principal stress lines will have maximum stiffness with the shortest length 17. As shown in Figure 5(b), in $\triangle OP_3P_2$, there is

$$\gamma=\pi-\alpha-2\theta \tag{2}$$

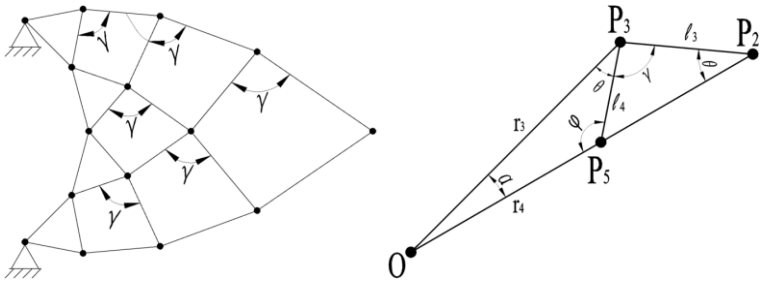

(a) Orthogonal principal lines design(γ equals $\pi/2$) 17 (b) $\triangle OP_3P_2$

Figure 5. Orthogonal relationships.

Then, combining Eq (1) with Eq (2), the orthogonality relationship expression can be developed with variables of γ, α and k. Where r_0 is the radius of the gear's root circle and $r_{n\text{-}1}$ is the radius of the hub, and n is the number of concentric circles.

$$\sin\gamma=\sin\alpha\cdot\sqrt{1-\frac{1}{k^2}\cos^2\left[\frac{1}{2}(\alpha+\gamma)\right]}+\frac{1}{k}\cos\alpha\cos\left[\frac{1}{2}(\alpha+\gamma)\right],\ k=(r_{n-1}/r_0)^{1/n} \tag{3}$$

In brief, when constructing the principal stress lines at the gear web, there are three steps: (a) Put

$r_{n\text{-}1}$, r_0 and α into Eq (3), set $\gamma = \pi/2$, then n can be calculated. (b) Put n, $r_{n\text{-}1}$ and r_0 into Eq (1) and the radius values of concentric circles will be calculated. (c) According to the design workflow as shown in Figure 3, the overall principal stress lines will be designed in the concentric circles.

3.3. Vibration control model

By offsetting the principal stress lines by a distance $2w$, a porous web will be generated. As shown in Figure 6(a), the porous web can be regarded as a loop with two kinds of holes, such as the inner holes ① and the outer holes ②. Where the inner holes are a series of analogous diamonds with the side lengths of l_1 - $2w$, …, l_n - $2w$ and with the angles of γ, the outer holes are a series of triangles with the side lengths of 1/2(l_n - $2w$) with the angles of γ. When $2w$ reaches a critical value with the decrease of $2w$, the outer holes' shape will change to pentagons with the additional corners from triangles, as shown in Figure 6(b).

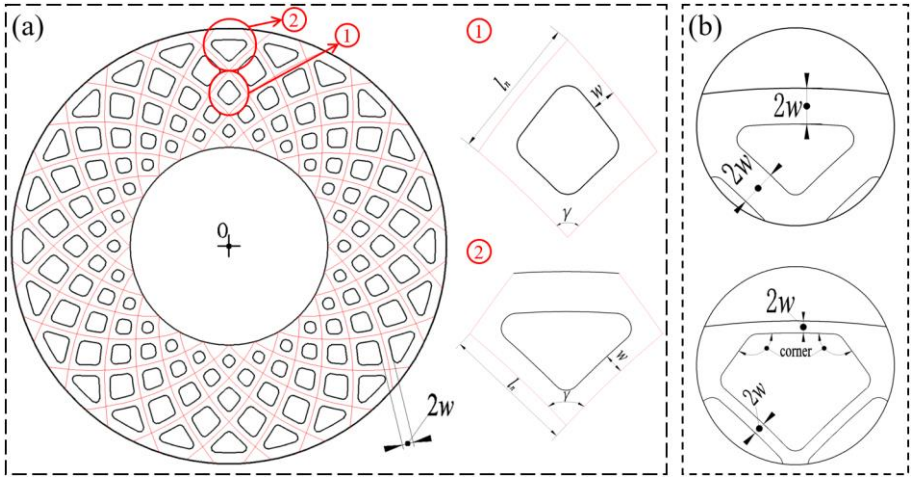

(a) Porous web, (b) Outer holes

Figure 6. Vibration control model.

In order to describe the relationship between the vibration amplitude of the porous web and $2w$, the vibration control model is proposed as follows. Where $A_{\max}$ is the maximum vibration amplitude of the porous web, $A_{0\max}$ is the maximum vibration amplitude of the solid web and z is the number of gear teeth.

$$A_{\max} = A_{0\max}\left\{1-\frac{z\cdot\sin\gamma\cdot\left[\sum_{i=1}^{n-1}(l_i-2w)^2+\frac{1}{2}(l_n-2w)^2\right]}{\pi\left(r_{outer}^2-r_{inner}^2\right)}\right\} \quad \begin{matrix}[2w]_{critical}<2w<\min[l_1,\cdots,l_n],\\ n\geq 2\end{matrix} \tag{4}$$

As shown in Eq (4), with the decrease of $2w$, the web's vibration area will decrease, thus to the decrease of $A_{\max}$. When $2w$ gets the critical value, $A_{\max}$ will reach the minimum.

When $2w$ exceeds the critical value, triangle outer holes change to pentagon outer holes with poor stiffness. As shown in Figure 7, in the same loading condition, the additional corners brought more than double stress increase and 0.4 times deformation increase for the outer holes. If the additional

corners were further enlarged, it could result in the structural destructive deformation and lead to the structural failure.

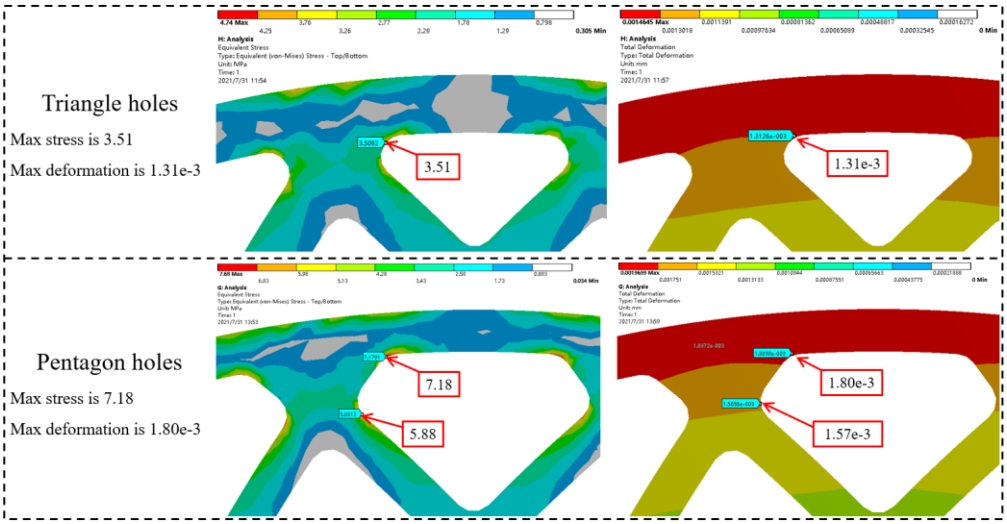

Figure 7. Simulation experiments in the same loading condition.

In addition, by Topology Optimization gear design method, it was verified that triangle was the optimal shape of the outer holes. In Topology Optimization, a serious of porous gears, with different number of holes, were obtained by changing the retention rate. As shown in Figure 8, although the holes number of the porous gears are different from each other, their outer holes are all triangle. It is due to the principle that Topology Optimization removed materials in the low stress region and preserved materials in the high stress region. In order to decrease the structural maximum stress, the outer holes of Topology Optimization gears are triangle. Therefore, with the decrease of $2w$, the porous web with triangle outer holes is the optimal shape.

Retention rate/%	40	50	60
Topology Optimization gears	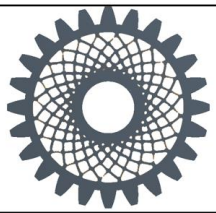	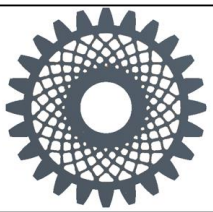	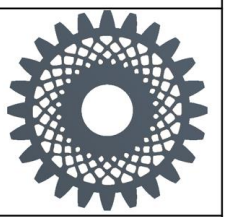
Retention rate/%	70	80	90
Topology Optimization gears	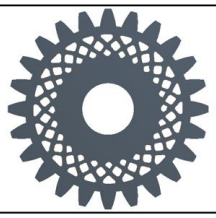	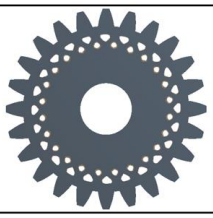	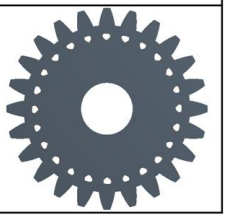

Figure 8. Topology Optimization gears with different retention rate.

$$
\begin{aligned}
&h_3 < \sin\frac{1}{2}\gamma \cdot (l_n - 2w) \\
&h_3 = h_1 - h_2 - 2w \\
&h_1 = r_{outer} - r_1 \\
&h_2 = w \Big/ \sin\frac{1}{2}\gamma \\
&r_1 = r_0 / k, k = (r_0 / r_{n-1})^{1/n}
\end{aligned} \tag{5}
$$

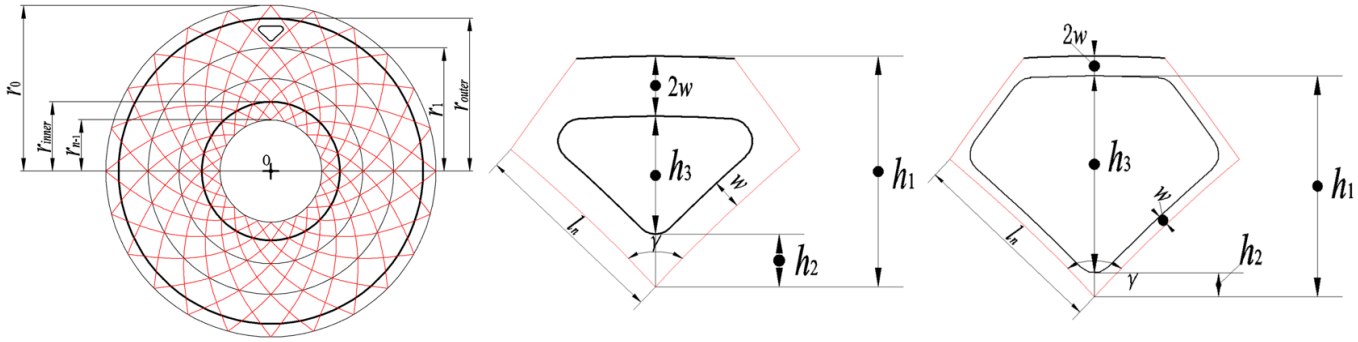

(a) Concentric circles for constructing principal stress lines, (b) Triangle holes, (c) Pentagon holes

Figure 9. Design method of triangle outer holes.

4. Experiment

4.1. Vibration control model

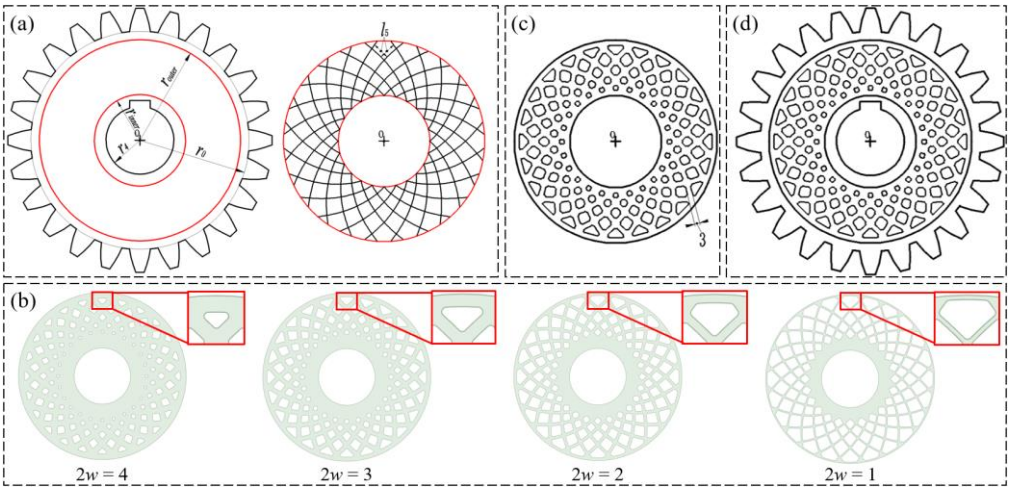

(a) Principal stress lines (b) Porous web with different 2*w* (c) Porous web with 2*w* of 3 (d) Novel gear 3

Figure 10. Design workflow of the novel gear 3.

According to the design parameters in Table 1, using photosensitive resin as the material, the novel gear was manufactured by Stereo lithography Apparatus. Referring to Section 3.2, the principal stress lines were constructed at the gear web as shown in Figure 10(a) and the length of each principal stress line was obtained as shown in Table 2. Then, put l_5(10.0), γ(90°), r_0(64.5), r_{outer}(59.5), n(5) into Eq (5), $2w > 2.9$ can be obtained. According to Eq (4), $A_{\max}$ would decrease with the decrease of $2w$. Hence set $2w = 3$ and the outer holes were still triangle, as shown in Figure 10(b). Therefore, by offsetting the principal stress lines at 3 *mm*, the porous web with the low vibration amplitude was generated, as shown in Figure 10(c). Finally, the gear teeth and hub were added to the porous web, the novel gear was then generated, as shown in Figure 10(d).

Table 1. Design parameters of the gear design.

Basic parameters	Value
Teeth number	24
Normal module/mm	6
r_0/mm	64.5
r_{outer}/mm	59.5
r_{inner}/mm	27
r_4/mm	20

In order to explore the influence of the web's porosity adjustment on gear vibration performance, the other three novel gears, with the web's porosity varying from 20 to 70% and $2w$ of 1, 2 and 4 *mm*, were also employed to the gear vibration experiment. In order to explore the loading performance of the novel gear, Topology Optimization gear, with the same web's porosity as the novel gear 3, was employed to the gear loading experiment. The above gears are as shown in Figure 11 and their mass comparison is as shown in Table 2.

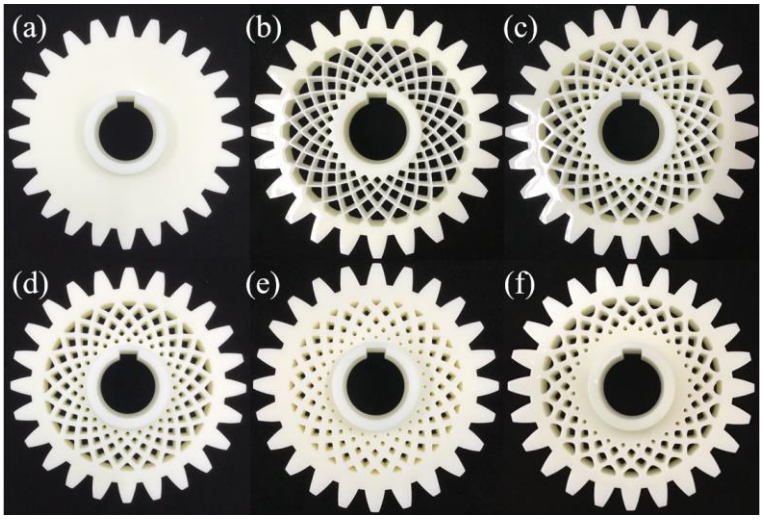

(a) Solid gear, (b) Novel gear 1, (c)Novel gear 2, (d) Novel gear 3, (e) Novel gear 4, (f) Topology Optimization gear

Figure 11. Experimental gears.

Table 2. Mass comparison for different gears.

	Mass/g	Web's porosity/%	Weight reduction/%
Solid gear	375.5	0	-
Novel gear 1 (2*w* is 1 mm)	229.1	69.5	39.0
Novel gear 2 (2*w* is 2 mm)	271.5	49.7	27.7
Novel gear 3 (2*w* is 3 mm)	298.5	36.7	20.5
Novel gear 4 (2*w* is 4 mm)	324.6	24.3	13.6
Topology Optimization gear	298.5	36.7	20.5

To verify the innovative gear web design method proposed, novel gear 3 was employed in vibration and loading experiment. In vibration performance experiment, there were six gear pairs being compared. Where S-S gear pair was composed of two solid gears, S-N*n* gear pair was composed of a solid gear and a novel gear with 2*w* of *n* mm where *n* equals 1, 2, 3, 4 respectively and S-T gear pair was composed of a solid gear and a Topology Optimization gear. Through analyzing the vibration signal of gear pair during the gear pair meshing, the frequency spectrums of different gear pairs were obtained. In the frequency spectrums, the vibration signals of the gear pair located at the dominant frequency with the highest amplitude. Where the amplitude value represents the vibration level. Therefore, using the vibration amplitude at dominant frequency as the criterion, gear vibration performance was evaluated. In loading performance experiment, using the motor's output torque till gear was broken as the criterion, gear loading performance was evaluated.

4.2. Experimental platform construction

The vibration performance of gears was detected by a vibration experimental platform, as shown in Figure 12(a). It mainly consists of a Transmission system as shown in Figure 12(b) and a Signal analysis system. The vibration signals were generated from the Transmission system, which consists of a Rotatable shaft, a pair of Shaft blocks, a Gear pairs and a motor with variable-frequency drive. In the aspect of installation, the central axis of the Gear pairs is required to be in the same horizontal position, and the center distance between the Gear pairs equals the gear diameter. In the aspect of signal processing, an accelerometer Sensor, adhered to the shaft block, was used to collect signals. A Spider-80XI module was used to process signals and the Crystal software then converted the time signal into the frequency spectrum. The gear loading performance was detected by a loading experimental platform, as shown in Figure 12(c). This platform was obtained by refitting the Transmission system, where the Rotatable shaft was replaced with a Fixed shaft and the Metal gear was installed on the Fixed shaft. Therefore, when the motor drove the gear to rotate, the Gear would not be able to rotate due to the constraint from the fixed Metal gear. During the gear loading experiment, the torque on the Gear increased with the increase of the motor's output torque. Therefore, by comparing the motor's output torque till the Gear was broken, the loading performance of the Gear would be compared.

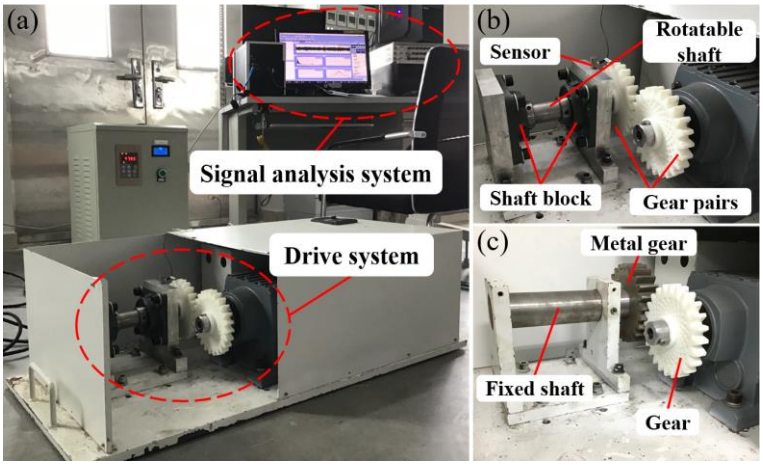

(a) Vibration experimental platform, (b) Transmission System, (c) Loading experimental platform

Figure 12. Experimental system construction.

5. Analysis of experimental results

5.1. Vibration performance analysis

As shown in Figure 13 and Table 3, the highest amplitude is 12.00 m/s^2, which is S-N_1. The lowest amplitude is 5.89 m/s^2, which is S-N_3. The amplitude of S-S is 8.35 m/s^2. The experimental result indicated that with the web's porosity adjustment, the innovative gear web design method would significantly reduce the gear vibration amplitude. Compared with solid gear, the vibration amplitude of novel gear 3 decreased by 29.46%.

Among these gear pairs, S-N_3, with the novel gear 3, has the lowest vibration amplitude, which verified the optimal shape of the porous web proposed in Section 2.3. In addition, the vibration amplitude of S-T, with the Topology Optimization gear, is 6.82 m/s^2, which is higher than S-N_3. It is because the holes of Topology Optimization gear are less than those of novel gear 3. For two porous gears with the same porosity, the decrease of holes (Novel gear 3 has 120 holes, Topology Optimization has 96 holes) caused the decrease of the noise travelling distance and noise travelling direction changes times, resulting in the decrease of noise energy loss. Therefore, the vibration amplitude of the Topology Optimization is higher than that of novel gear 3.

Table 3. Vibration experiment results.

	Web's porosity/%	Frequency /Hz	Vibration amplitude/m/s^2	Vibration reduction/%
S-S	0	375.00	8.35	0
S-N_1	69.50	337.50	12.00	-
S-N_2	49.70	406.25	8.05	3.59
S-N_3	36.70	231.25	5.89	29.46
S-N_4	24.30	418.75	7.01	16.05
S-T	36.70	181.25	6.82	18.32

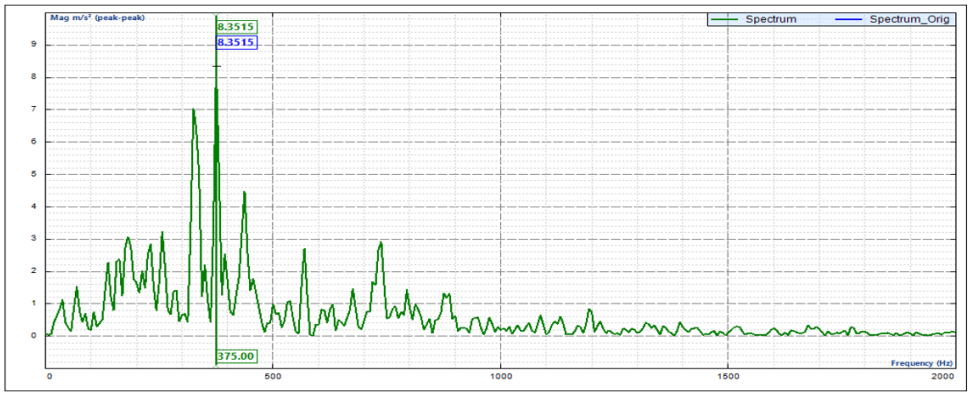

(a) S-S gear pair

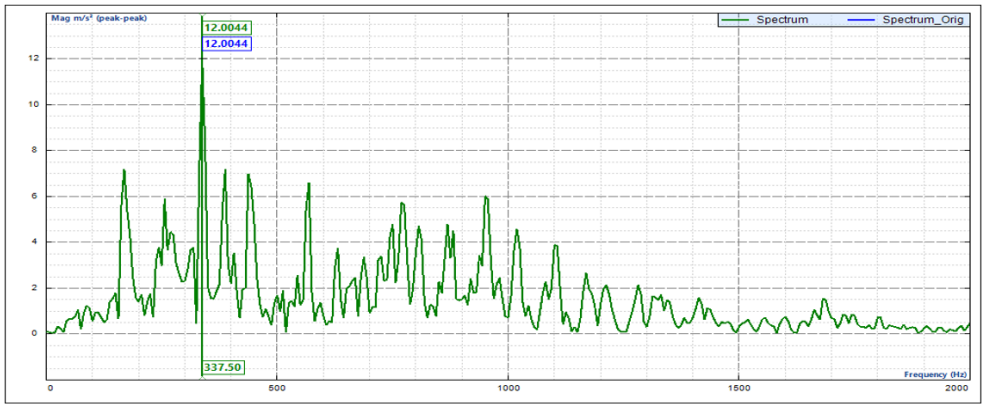

(b) S-N1 gear pair

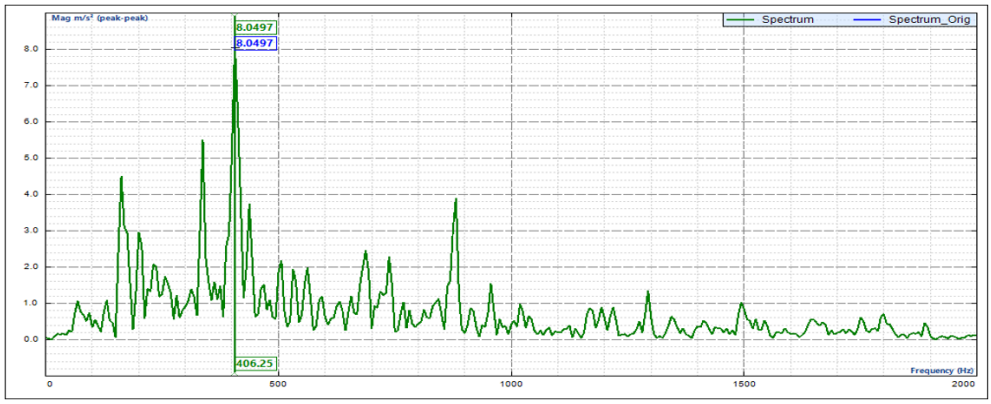

(c) S-N2 gear pair

continued on next page

Figure 13. Frequency spectrums of acceleration for different gear pairs.

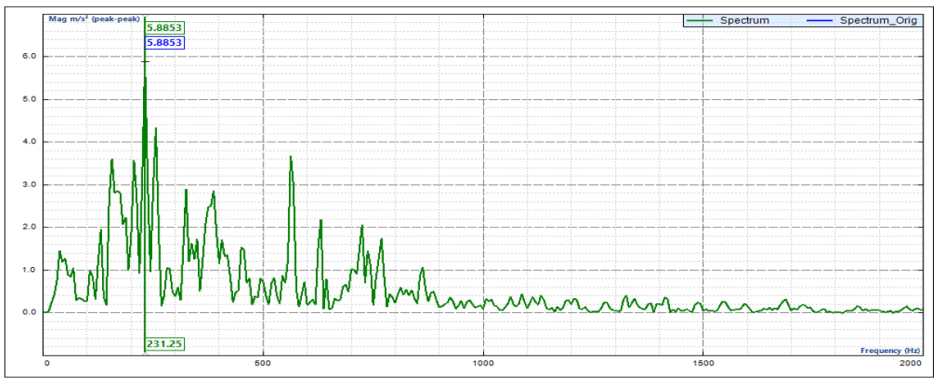

(d) S-N3 gear pair

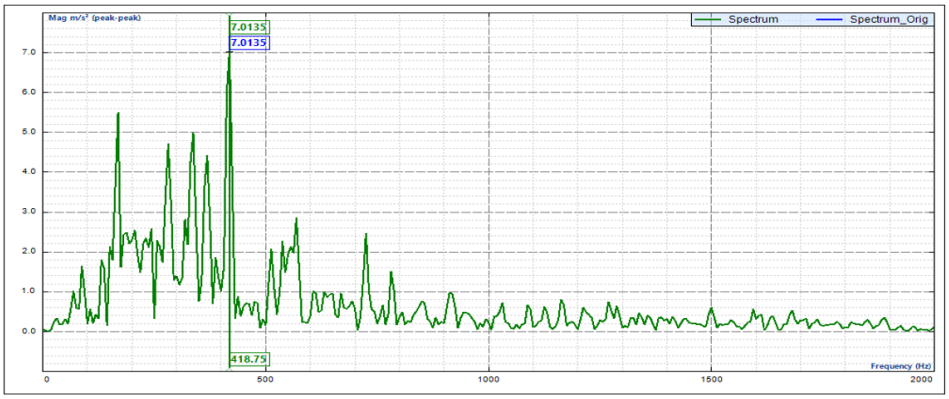

(e) S-N4 gear pair

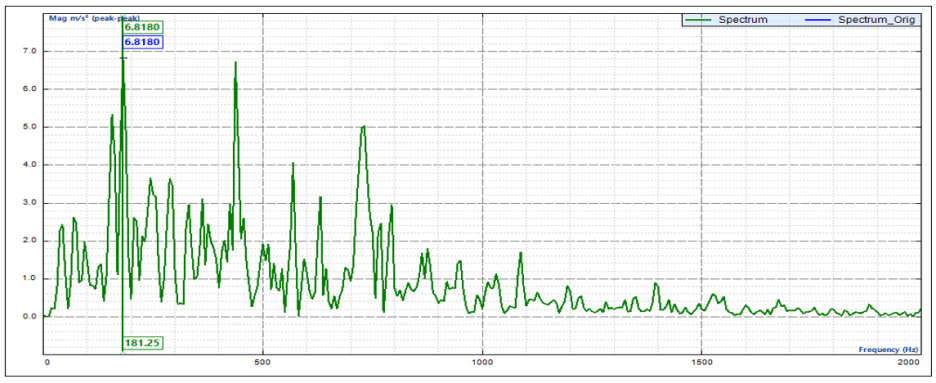

(f) S-T gear pair

Figure 13. Frequency spectrums of acceleration for different gear pairs.

As shown in Figure 14, with the increase of the web's porosity, the vibration amplitude of the gear decreased and the vibration performance was improved accordingly. When the web's porosity got to a critical value, the vibration amplitude was the lowest and the vibration performance reached the optimum. However, when the web's porosity exceeded the critical value, the vibration amplitude began to increase again and the vibration performance was impaired accordingly. This is mainly because the

excessive web's porosity decrease caused its insufficient stiffness, resulting in the vibration performance reduction. Therefore, when adjusting the web's porosity to improve the gear vibration performance, it should consider the balance between the web's porosity and its structural stiffness.

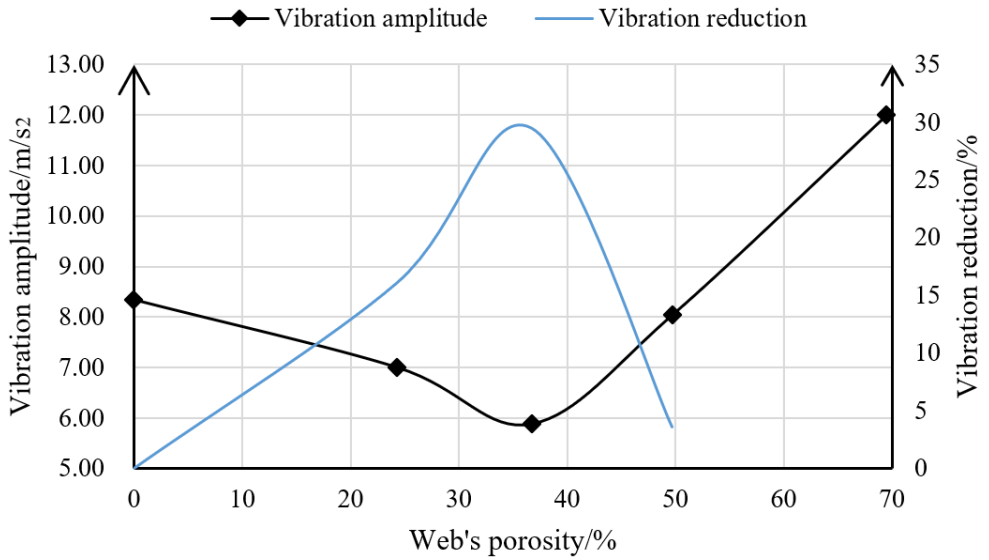

Figure 14. The relationship between the web's porosity and gear's vibration amplitude.

5.2. Loading performance analysis

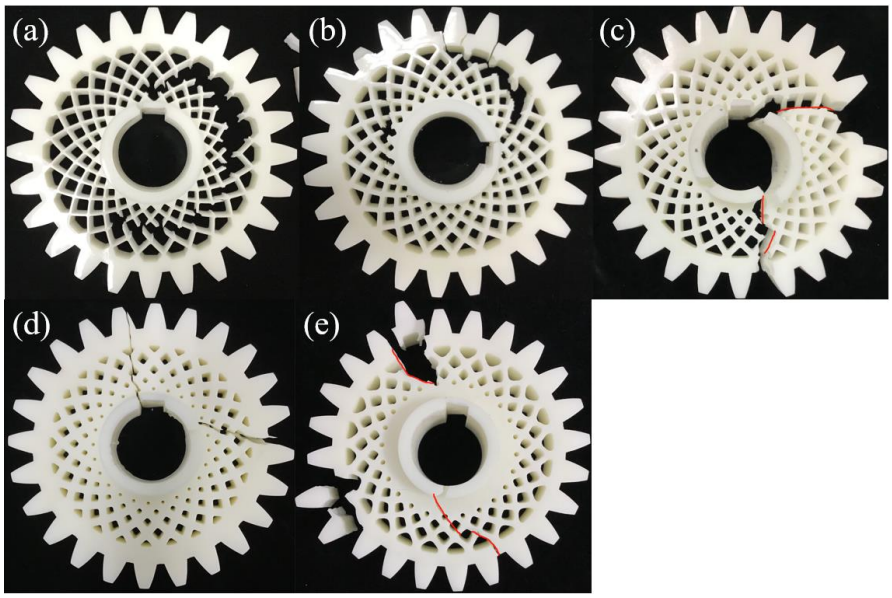

(a) Novel gear 1 (b) Novel gear 2 (c) Novel gear 3 (d) Novel gear 4 (e) Topology Optimization gear

Figure 15. The fracture conditions of different gears.

In this section, four novel gears ($2w$ = 1, 2, 3, 4) were compared with their loading performance and the experimental results are shown in Table 4. As shown in Figure 15(a),(b), when

$2w$ = 1 and $2w$ = 2, the gears' fractures appeared in the outer holes and their loading performance were poor. As shown in Figure 15(c),(d), when $2w$ = 3 and $2w$ = 4, the gears broke completely and their loading performance were better. The experimental result indicated with the decrease of $2w$, the novel gears with triangle outer holes performed better than those with pentagon outer holes, which verified the optimal shape of the porous web proposed in Section 3.3.

According to the innovative gear web design method proposed, novel gear 3 was constructed. In order to verify its loading performance, Topology Optimization gear with the same porosity was employed in the contrast experiment. As shown in Figure 15(c),(e), the gears' fractures (see red lines) both spread along their holes and their loading performance were the same. Referring to Section 3.1, Topology Optimization gear, whose materials are distributed along the structural principal stress lines, is characterized by the minimal weight and the maximum stiffness. Therefore, the structural principal stress lines design method proposed was verified and novel gear 3 possessed a sufficient loading performance.

Table 4. Loading experiment results.

	Torque/N • m
Novel gear 1 ($2w$ is 1 mm)	1.4
Novel gear 2 ($2w$ is 2 mm)	2.8
Novel gear 3 ($2w$ is 3 mm)	4.2
Novel gear 4 ($2w$ is 4 mm)	4.5
Topology Optimization gear	4.2

6. Conclusions

In order to achieve weight, vibration and noise level reduction in the current gear design, this paper proposed a porous gear web design method based on the principal stress lines. Based on the results in gear vibration and loading experiments, some conclusions are as follows:

(I) By designing the gear web as the porous structure whose materials are distributed along its principal stress lines, the gear can reduce its weight while maintaining sufficient loading performance.

(II) By changing the web's porosity under the vibration control model proposed, the vibration amplitude of the gear can be effectively decreased.

(III) Compared with the solid gear, the novel gear was lighter by 20.50% with a 29.46% vibration amplitude reduction, which means that this method realized the integrated gear web design of weight and vibration reduction.

Acknowledgments

This study was funded by National Natural Science Foundation of China (No. 51775273), Jiangsu Province Science and Technology Support Plan Project (No.BE2018010-2), Open-End Fund for Graduate Students (Nanjing University of Aeronautics and Astronautics) (No. kfjj20200512), National Defence Basic Scientific Research Program of China (No. JCKY2018605C010), Aeronautical Science Foundation of China (No. 2020Z049052002), National Key Laboratory of Science and Technology on Helicopter Transmission(Nanjing University of Aeronautics and Astronautics)(No. HTL-A-19G012).

Conflict of interest

The authors declare that there is no conflict of interests regarding the publication of this paper.

References

1. R. Ramadani, M. Kegl, J. Predan, A. Belšak, S. Pehan, Influence of cellular lattice body structure on gear vibration induced by meshing, *J. Eng. Mech.*, **64** (2018), 611–620.
2. M. Faggioni, F. Samani, G. Bertacchi, F. Pellicano, Dynamic optimization of spur gears, *Mech. Mach. Theory*, **46** (2011), 544–557.
3. S. Li, Experimental investigation and FEM analysis of resonance frequency behavior of three-dimensional, thin-walled spur gears with a power-circulating test rig, *Mech. Mach. Theory*, **43** (2008), 934–963.
4. J. Smith, Gear noise and vibration, *Marcel Dekker*, (2003), 1–12.
5. S. Ghosh, G. Chakraborty, On optimal tooth profile modification for reduction of vibration and noise in spur gear pairs, *Mech. Mach. Theory*, **105** (2016), 145–163.
6. R. Handschuh, G. Roberts, R. Sinnamon, B. Stringer, D. Dykas, W. Kohlman, et al., Hybrid gear preliminary results-application of composites to dynamic mechanical components, *Nasa Tm.*, (2012), 217630.
7. W. Xiao, Y. Huang, H. Jiang, J. Lina, Effect of powder material on vibration reduction of gear system in centrifugal field, *Adv. Powder. Technol.*, **294** (2016), 146–158.
8. R. Ramadani, A. Belsak, M. Kegl, J. Predan, S. Pehan, Topology optimization based design of lightweight and low vibration gear bodies, *Int. J. Simul. Model.*, **17** (2018), 92–104.
9. D. Li, W. Liao, N. Dai, G. Dong, Y. Tang, Y. Xie, Optimal design and modeling of gyroid-based functionally graded cellular structures for additive manufacturing, *Comput. Aided. Design.*, **104** (2018), 87–99.
10. J. Zhou, J. Su, Ansys workbench detailed analysis of finite element examples (dynamics), *Posts & Telecom Press*, (2019), 81–110.
11. N. Aage, E. Andreassen, B. Lazarov, O. Sigmund, Giga-voxel computational morphogenesis for structural design, *Nature*, **550** (2017), 84–86.
12. J. Zhang, B. Wang, F. Niu, G. Cheng, Design optimization of connection section for concentrated force diffusion, *Mech. Based. Des. Struc.*, **43** (2015), 209–231.
13. D. Gao, On Topology optimization and canonical duality method, *Comput. Method. Appl. M.*, **341** (2018), 249–277.
14. T. Kwok, Y. Li, Y. Chen, A structural topology design method based on principal stress line, *Comput. Aided. Design*., **80** (2016), 19–31.
15. G. Xu, N. Dai, Michell truss design for lightweight gear bodies, *Math. Biosci. Eng.*, **18** (2021), 1653–1669.
16. R. E. Skelton, M. C. de Oliveira, Optimal tensegrity structures in bending: the discrete Michell truss, *J. Franklin. Inst*., **347** (2010), 257–283.
17. A. Mazurek, W. Baker, C. Tork, Geometrical aspects of optimum truss like structures, *Struct. Multidiscip. Optim.*, **43** (2010), 231–242.